Magnetic Interaction of Super-Earths with their Host Star and Planet Composition

by

Ana-Maria Piso

Submitted to the Department of Physics
in partial fulfillment of the requirements for the degree of

Bachelor of Science in Physics

at the

MASSACHUSETTS INSTITUTE OF TECHNOLOGY

June 2010

Author .....
Department of Physics
May 07, 2010

Certified by .....
Paola Rebusco
Pappalardo Fellow
Thesis Supervisor

Certified by .....
Sara Seager
Associate Professor
Thesis Supervisor

Accepted by .....
David Pritchard
Senior Thesis Coordinator, Physics Department

Magnetic Interaction of Super-Earths with their Host Star and Planet Composition

by

Ana-Maria Piso

Submitted to the Department of Physics
on May 07, 2010, in partial fulfillment of the
requirements for the degree of
Bachelor of Science in Physics

Abstract

We study the magnetic field and the planet-star interactions of super Earths, extra-solar planets with masses between 1 and 10 times the mass of the Earth. We first present a model of the magnetic field of a super Earth, the dynamo model. We then list and explain several mechanisms through which magnetic energy can be released, as well as various ways through which the power dissipated can be observed. We apply our model to two recently discovered super Earths, CoRoT 7-b and GJ 1214 b. We find that emission from CoRoT 7-b is very low and thus unlikely to be observable, while emission from GJ 1214 b may be detectable with current instruments and its measurement can provide information regarding the internal composition of the planet. Further on, we discuss some special cases for detection, such as M and Ap type stars. We conclude our thesis with a generalization of our results and guidelines for future developments.

Thesis Supervisor: Paola Rebusco
Title: Pappalardo Fellow

Thesis Supervisor: Sara Seager
Title: Associate Professor

Acknowledgments

I would like to thank the following people for their contribution to this project:

Doctor Paola Rebusco, for being involved in every step of this thesis. None of this would have been possible without her constant advice and insights, her almost daily feedback and proof reading, her encouragement, patience and enthusiasm.

Professor Sara Seager, for all her support and advice throughout this past year, and for helping me shape my future as a researcher. I am grateful for the opportunity to work with and learn from her.

Doctor Mike Stevenson, for his skillful proofreading and his insightful suggestions.

I would also like to thank Professor Bruno Coppi, Doctor Elena Gallo and Professor Caleb Scharf for providing me with conversations and references essential to my understanding and analysis of this work.

A special thank you to Professor Edmund Bertschinger, for his help and guidance in my past two years as a UROP student.

Finally, I would like to thank my loved ones for their constant words of encouragement, for believing in me, and for always being there for me, willing to listen to my complaints and offer me a hug when things get tough.

Contents

List of Figures

List of Tables

Chapter 1

Introduction

Do other Earths exist? And if so, do they harbor life? This is one of the main questions planetary science is aiming to answer. As of today, more than 400 planets have been detected outside the solar system. The majority of them have been discovered by Doppler techniques, which measure the star's line-of-sight motion as the star orbits the planet-star common center of mass. Most of the extrasolar planets, or exoplanets, that have been detected are giant planets, with much larger masses than that of the Earth. Hence, the next and possibly more fascinating step is discovering planets with masses close to the Earth mass, the so called super Earths. At the present time, the detection and study of exoplanets is a hot topic in astronomy and astrophysics, especially since several super Earths have recently been detected and new missions will soon discover more (e.g. Kepler) [17].

1.1 History

The first planets outside the solar system were detected in 1992 by Aleksander Wolszczan and Dale Frail. They discovered three planets orbiting the pulsar PSR1257+12. However, the first exoplanet orbiting a main sequence star, 51 Pegasi, was discovered in 1995 by Michel Mayor and Didier Queloz. It was therefore named 51 Pegasi b [1].

[1]The nomenclature convention for exoplanets is the following: the first planet discovered in a star system receives the name of the star followed by the letter 'b' (for example, the first planet in the star system 51 Pegasi was named 51 Pegasi b). The following planets receive the letters 'c', 'd',

1.2 Detection Techniques

Currently, there are several methods to detect exoplanets. We briefly summarize them and explain their limitations.

1.2.1 Direct detection

Detecting an exoplanet directly is very difficult, due to the fact that the parent star emits much more light than the planet, making it impossible to be seen in visible light. There are several methods to detect a planet, such as using infrared radiation rather than visible light, or using a coronograph that blocks the direct light from the star. Although direct detection is sometimes the only way to assess important physical parameters of the planet, it is an enormous challenge. Alternatively, there are several indirect methods of exoplanet detection that can provide useful insight into exoplanet properties. The indirect methods assess the existence and features of an exoplanet by examining the effect on the parent star or observations thereof.

1.2.2 Doppler methods (Radial velocity tracking)

The presence of an exoplanet causes the parent star to move in a small orbit around the common center of mass. The velocity with which the star moves as seen along the line of sight of an observer from Earth is called radial velocity. The star will move towards, then away from the Earth as it completes an orbit, and hence cause the lines in the spectrum of the star to undergo Doppler shift. This effect can be detected on Earth by high-precision spectrographs. Such measurements can yield, for example, lower bounds on the mass of the planet. Currently, one of the most successful detectors is called HARPS (High Accuracy Radial Velocity for Planetary Searcher) and is mounted on the 3.6 m ESO (European Southern Observatory) telescope from La Silla, Chile.

'e' etc. as they are discovered.

1.2.3 Transit method

If a planet passes (transits) between its host star and Earth, the apparent brightness of the star as observed from Earth decreases. This effect can be measured using photometry. The transit method can reveal important information about the atmosphere of the planet. It is used, for example, by the Kepler mission launched by NASA in 2009 to search for planets in the Cygnus constellation, or by the COROT mission led by the French Space agency and the European Space Agency [5].

1.2.4 Pulsar Timing

A pulsar emits radio pulses regularly as it rotates. If a planet is orbiting a pulsar, it will affect the timing of the emitted pulses. This is how the first exoplanets mentioned in section 1.1 were detected.

1.2.5 Gravitational lensing

The gravitational attraction of a star will bend and amplify the light coming from another distant star, acting like a magnifying lens. If, however, there is a planet orbiting the lens star, the light curve of the distant star will change slightly - it will contain an additional peak. The size and shape of the secondary peak will depend on the mass and distance of the planet from the host star. This method was used, for example, to detect the extra solar planet OGLE 2003-BLG-235.

1.2.6 Astrometry

Astrometry is used to observe the position in the sky of a star and how that position changes over time - if a star is orbited by a planet, the star itself will move in a small orbit around the center of mass of the planet-star system. This method is thus similar to the radial velocity method. So far there have not been any successful detections using astrometry.

1.3 Current discoveries and planetary parameters

As of March 23, 2010, 442 extra solar planets have been confirmed [4]. A plot of the mass of the planets as a function of their radius, as well as the detection methods, is shown in Fig. A-1. Most of the planets discovered so far are large and they orbit very close to their host star. This is due to the fact that large planets are usually easier to detect. Such planets, of roughly Jupiter-like masses, are called 'hot Jupiters'. However, several smaller planets have been discovered in the past couple of years (e.g. CoRoT 7-b, Gliese 581 e, GJ 1214 b). The planets with masses between 1 and 10 Earth masses are called 'super Earths'.

If a planet is found through the radial velocity method, its orbital inclination i (the angle between the rotation axis of the planet and the planetary orbit) is unknown, and hence it is only possible to detect its minimum mass, $M \sin i$. However, the angle i has, statistically, an average of $\pi/4 = 0.785$, so the minimum mass estimates will generally be close to the true mass of the planet [10]. Additionally, if a planet is detected by the transit method, then its inclination angle is known, and so the true mass of the planet can be accurately determined.

The surface temperature of an exoplanet can be estimated from the intensity of the light it receives from its host star, or from variations in the infrared radiation received as the planet orbits around its parent star and is eclipsed by it.

The average density of a planet can be determined once we know its mass and radius. The density can give us some information regarding the internal composition of the planet. For example, planets with low average density are assumed to be composed mainly of hydrogen and helium, which is the case for hot Jupiters. Planets with a medium average density are likely to have water as a predominant element, while planets with a high average density are believed to have a rocky structure, similar to that of the Earth. The exact structure and composition of a planet are difficult

to estimate; however, more knowledge regarding the internal structure and the atmosphere of a planet can give information regarding its habitability (its capacity to sustain life).

1.4 Planet-star interactions

In this section we discuss possible interactions between exoplanets and their host stars. The existence of a planet around a star can affect the outer atmospheric layers of the star or the coronal activity [11]. We can classify the star-planet interactions into tidal interaction and magnetic interaction.

1.4.1 Tidal interaction

The tidal interaction between a planet and its host star arises as an effect of the gravitational acceleration caused by the planet. This gravitational acceleration varies in strength and orientation along the surface of the star, affecting the motions and flow fields in the atmospheric layers of the star [11]. If the orbital period of the planet and the rotational period of the stars are different, the variation of the gravitational force will cause stellar tidal bulges (expansions and subsequent contractions of the outer layers of the star due to different accelerations on the side nearest to the planet and on the side farthest to the planet). Since the flow velocities increase in these tidal bulges, more energy will be released, resulting in an enhanced level of stellar activity. [11] proposes a model for estimating the strength of the tidal interaction between extrasolar giant planets and their host stars. In this thesis, however, we will not discuss tidal interaction. This is mostly due to the fact that most extrasolar planets have an orbital period very close or equal to the rotational period of their host star, and so tidal interactions can be neglected in this situation. Instead, we will focus on the magnetic interaction between a planet and its parent star.

1.4.2 Magnetic interaction

Another important type of interaction between a planet and a star is the interaction between the magnetic fields of the two celestial bodies. This interaction usually occurs at the surface of the magnetosphere of the planet (the region of space to which the planetary magnetic field is confined by the stellar wind plasma blowing outward from the host star). The magnitude of the interaction is mainly determined by magnetic reconnection, which will be discussed in more detail in section 2.3.1. The magnetic interaction between a planet and its host star will lead to the release of magnetic energy that will be emitted in various forms of electromagnetic radiation (see section 2.5). The magnetic interaction between giant exoplanets (hot Jupiters) and their parent star has been studied in detail ([11], [38], [19], [13]). We will discuss it in more detail in Chapter 2.

1.5 Motivation

There are currently several models of the magnetic interaction between extrasolar giant planets and their host stars. However, the magnetic interaction between super Earths and their parent star has not been investigated yet. This is mainly due to the fact that planets with a mass similar to that of Earth have only recently been discovered. Additionally, super Earths have a relatively small mass and radius (compared to hot Jupiters), which will usually cause the magnetic field to have a smaller strength that in the case of hot Jupiters. Therefore, we expect the strength of the magnetic interaction for super Earths to be much smaller than in the case of hot Jupiters, and hence not easily detectable. However, this is not always the case. As we will see in chapter 3, emission from the super Earth GJ 1214 b is in the detectable range. Furthermore, the development of instruments with higher capabilities and sensitivity will make it possible to observe weaker interactions. Creating a magnetic interaction model for super Earths and comparing it with observations can provide us with essential information regarding the internal structure and composition of these planets. Among others, it could give important pieces of information in determining

whether a super Earth can be habitable or not, which is one of the main questions that planetary science is trying to answer.

Chapter 2

Magnetic Interaction Model

In this chapter we review the models for magnetic interaction between an extrasolar planet and its host star. We first present the general case, after which we apply it to the particular instance of super Earths. We model the magnetic field of the planet as a dynamo and briefly explain the conditions under which the dynamo can exist. We then model the magnetic interaction between the planet and its host star, focusing on different types of mechanisms through which power can be released. All the results we present are based on scaling arguments. Lastly, we relate our model to observations.

2.1 Planetary Magnetic Field

2.1.1 Dynamo model

The dynamo model is a mechanism through which a celestial body, such as a star or a planet, can generate a magnetic field. This process involves rotation of, convection in and electrical conduction in the celestial body. It is a complex process that is not fully understood.

The planetary core represents the innermost layer of a planet. For some planets, it can be separated into an inner, solid core and an outer, liquid shell. A magnetic field can be generated by the movement (conduction) of charged particles in the outer shell

of the core of the planet. In order to produce a current, the outer shell needs to be made of a conducting material: it can be an iron-nickel composition, as is the case for the Earth, metallic hydrogen (Jupiter), or even a salt-water composition (Ganymede [18]). Due to differences in temperature and composition, convective motions are created in the outer shell. These convective motions produce an electromotive force and the associated currents and fields, which, by induction, give rise to a reinforced magnetic field. This field then undergoes rotation and convection, resulting in a positive feedback cycle. In order for the magnetic field to be strong enough, the currents need to flow fast enough and exhibit convection. If a planet rotates too slowly or its core is too viscous, a strong magnetic field cannot be created. As such, the strength of the magnetic field of a planet can give us information regarding its internal structure. An analogy between the planetary dynamo and the disc dynamo can be seen in Fig. A-2.

The magnetic field in the case of a dynamo is described by the induction equation [39]:

$$\frac{\partial \mathbf{B}}{\partial t} = \lambda \nabla^2 \mathbf{B} + \nabla \times (\mathbf{v} \times \mathbf{B}), \tag{2.1}$$

where $\mathbf{B}$ is the magnetic field vector, $\mathbf{v}$ is the fluid velocity relative to the rotating frame of reference of the planet, and λ is the magnetic diffusivity [39] and is defined as $\lambda = 1/\mu_0 \sigma$, where μ_0 is the vacuum permeability and σ is the electrical conductivity. The first factor on the right hand side of the above equation is the conduction term, while the second factor is the convection term.

We are interested in the conditions for which a planetary dynamo exists. We follow here the exposition in [39]. First off, we know that if the dynamo is suddenly stopped (there is no more fluid motion), the magnetic field decays in time. The time scale of this free decay can be approximated as [39]

$$\tau \sim \frac{L^2}{\pi^2 \lambda}, \tag{2.2}$$

where L is a characteristic length of the field. In our calculations, we take $L \sim r_0$, where r_0 is the radius of the planetary core. As such, for a constant decay time (typical values are 10^4 years for the Earth), we obtain a relation between the radius of the conducting region r_0 and the electrical conductivity σ of the core:

$$r_0 \sim \sigma^{-1/2}. \tag{2.3}$$

Furthermore, we assume that the heat flow from the core is all being transported to the dynamo region rather than absorbed. In this approximation, the total heat flow at a radius r from the center of the planet is given by

$$F_{total}(r) = -\rho_c C_p r \frac{dT_c}{dt}\frac{1}{3}, \tag{2.4}$$

where ρ_c is the mean core density, C_p is the specific heat and T_c is the mean temperature of the core. The condition for thermal convection (and hence the existence of a dynamo regime) is that the heat flow defined in equation (2.4) must be higher than the heat flow carried by conduction along an adiabat, defined as

$$F_{cond,ad} = 4\pi G \rho_c r k \alpha T / C_p, \tag{2.5}$$

where k is the thermal conductivity, α is the coefficient of thermal expansion and G is the gravitational constant. In order to relate the above mentioned quantities to electrical conductivity, we will use the Wiedemann-Franz law [39], an empirical law named after Gustav Wiedemann and Rudolph Franz, which states that the ratio of the thermal and electrical conductivity in a metal is proportional to the temperature. The proportionality constant is called the Lorentz number and is given by

$$L = \frac{k}{\sigma T} = \frac{\pi^2}{3}\left(\frac{k_B}{e}\right)^2 \approx 2 \times 10^{-8} W\Omega/K^2, \tag{2.6}$$

where k_B is Boltzmann's constant and e is the elementary charge. This, together with the dynamo existence condition, implies an upper bound for the electrical conductivity

in order for conduction to be possible. For nominal parameter choices, this upper bound is roughly equal to the electrical conductivity in the Earth core [39]. It is important to mention that the Wiedemann-Franz law is only valid for terrestrial planets - for ice planets, the heat flow along the adiabat is much higher than the actual heat flow [39]. From this upper bound and from the proportionality in equation (2.2) we can obtain conditions for the existence of a dynamo, as a function of the core radius r_0 and the electrical conductivity σ of the core. Numerical estimations for super Earths will be presented in Chapter 3.

2.1.2 Induction fields

Apart from a magnetic field produced by a dynamo, a planet can also have an induction field (a magnetic field produced by an external field, e.g. another celestial body). For an external field that varies with angular frequency ω and for a thin conducting shell of the planet, of radius R and thickness d, a strong induction will exist if $(\lambda/\omega)^{1/2} < (Rd)^{1/2}$ [39]. In this thesis we neglect the induction fields.

2.2 Magnetic field strength

By Lenz's law, the Lorentz force created by the currents induced by core motion will act to oppose the rotation of the core, quantified by the Coriolis force. Strong planetary dynamos work in an equilibrium regime, and hence the Coriolis Force $\sim$ the Lorentz Force [32], with the ratio between the two forces being defined as the Elsasser number: $\Lambda \equiv |\mathbf{F_{cor}}|/|\mathbf{F_{lor}}|$.

In the fluid frame, the Coriolis force per unit volume is given by:

$$\mathbf{F_{cor}} = 2\rho\mathbf{v} \times \mathbf{\Omega} \rightarrow |\mathbf{F_{cor}}| = 2\rho v\Omega, \tag{2.7}$$

where ρ and $\mathbf{v}$ are the density and the velocity of the fluid, respectively, and Ω is the angular velocity.

The Lorentz force per unit volume is given by:

$$\mathbf{F_{lor}} = \mathbf{j} \times \mathbf{B} \rightarrow |\mathbf{F_{lor}}| = jB. \tag{2.8}$$

But $j = \sigma E = \sigma v B^2$, where σ is the electrical conductivity of the fluid and E is the electric field. As such, we obtain that the Elsasser number is given by

$$\Lambda = \frac{B^2}{2\Omega_0 \rho_0 \mu_0 \lambda}. \tag{2.9}$$

We define $\lambda \equiv 1/\mu_0 \sigma$. Also, in this case, the density ρ will be the density at the surface of the planetary metallic core of radius r_0: $\rho = \rho(r_0) \equiv \rho_0$. We therefore obtain from equation (2.9) that the magnetic field strength is given by

$$B = \sqrt{2\Omega \mu_0 \rho_0 \lambda \Lambda}. \tag{2.10}$$

Since for the dynamo regime $|\mathbf{F_{cor}}| \sim |\mathbf{F_{lor}}|$, we expect the Elsasser number to be of order 1 [34]. In addition, we know that the Elsasser number does not vary much in known planets ($\Lambda \sim 1$ for the Earth, $\Lambda \sim 0.01$ for Uranus and Neptune). Since B changes as $\sim \Lambda^{1/2}$, we can see that an Elsasser number between the 0.01 and 1 will change the strength of the magnetic field by at most one order of magnitude. However, since we will encounter many other uncertainties in our subsequent estimations, we can incorporate the uncertainty of the Elsasser number in the other uncertainties. As such, we consider from now on that $\Lambda = 1$. We obtain that the magnetic field strength at the surface of the core is given by

$$B = \sqrt{2\Omega \mu_0 \rho_0 \lambda}. \tag{2.11}$$

Since we are using a dynamo model, the magnetic field is represented by a dipole,

with intensity in polar coordinates given (to first order) by

$$B(r,\theta) = \frac{M_D}{r^3}(1 + 3\sin\theta), \tag{2.12}$$

where r and θ are the polar coordinates centered on the planet and M_D is the dipolar magnetic moment and is given by

$$M_D = Br_0^3, \tag{2.13}$$

where r_0 is the radius of the metallic core.

2.3 Star-Planet Magnetic Interaction

In this section we discuss different mechanisms of power release due to the planet-star interaction, as well as the observational means by which such energy releases can be detected.

2.3.1 Magnetic reconnection

Magnetic reconnection is the fundamental mechanism in a plasma through which magnetic field lines, normally attached to the plasma, become detached, break (disconnect) and rejoin (reconnect). The magnetic fields can annihilate each other, causing the plasma to follow a trajectory along the weaker field, at a velocity called the Alfven speed. Essentially, magnetic reconnection is a topological restructuring of a magnetic field due to the change in connectivity of the field lines. During this process, magnetic energy is released as heat, plasma kinetic energy or fast particle energy. Magnetic reconnection occurs in solar flares, coronal heating geomagnetic storms and many other dynamical processes in astrophysical objects.

The magnetic reconnection between the magnetic field lines of a planet and the magnetic field associated with the wind of the host star takes place at the magnetopause

of the planet. The magnetopause is the surface between the magnetosphere of the planet (the region of space to which the planetary magnetic field is confined by the stellar wind plasma blowing outward from the host star) and the surrounding plasma, on which the magnetic pressure of the planet is equal to the ram pressure of the stellar wind. From [22] and [19], the power released due to reconnection can be approximated as:

$$P = V B_{MP}^2 R_{MP}^2 \text{ erg/s}, \tag{2.14}$$

where V is either the radial or tangential component of the stellar wind velocity (see the paragraphs below), B_{MP} is the magnetic field strength at the magnetopause and R_{MP} is the radius of the magnetopause. This expression for the power dissipated can be obtained by taking into account that the energy dissipated through reconnection is a fraction of the total energy, which is the energy density $B^2/8\pi$ integrated over the volume. As such, the power dissipated can be expressed as a fraction of the energy density integrated over the changing volume $r^2 v$, where r is the radial distance and v is the stellar wind velocity. We integrate over the magnetosphere and therefore obtain that the dissipated power is proportional to $B_{MP}^2 R_{MP}^2 V$, explaining equation (2.14).

Before proceeding with this model, we need to explain the conditions under which this interaction is significant and therefore can potentially be detectable. We will show here that the strength of the interaction will depend, among other variables, on the distance between the planet and the star relative to the Alfven radius.

Alfven radius

The Alfven radius r_A is the distance from the star for which the ram pressure is balanced by the magnetic pressure [27]:

$$\rho_w V^2|_{r=r_A} = \frac{B_r(r_A)^2}{8\pi}, \tag{2.15}$$

where ρ_w is the stellar wind density and $B_r(r_A)$ is the radial magnetic field of the host star at $r = r_A$. The mass loss rate of the star is related to the stellar wind density and velocity by

$$\dot{M(r_A)} = 4\pi r_A^2 \rho_w V. \tag{2.16}$$

From equations (2.15) and (2.16) we find that the Alfven radius is given by

$$r_A = \sqrt{\frac{V\dot{M(r_A)}}{B_r^2}}. \tag{2.17}$$

Furthermore, $B_r(r_A)$ can be expressed as

$$B_r(r_A) = B_*\left(\frac{R_*}{r_A}\right)^3, \tag{2.18}$$

where B_* is the magnetic field strength at the surface of the star and R_* is the radius of the star. We therefore obtain from equations 2.17 and 2.18 the following expression for the Alfven radius:

$$r_A = \frac{V^2\dot{M(r_A)}^2}{B_*^4 R_*^3}. \tag{2.19}$$

The typical value of the Alfven radius of the Sun is $r_A \sim 15R_{sun} = 0.07$ AU [30], depending on the solar activity.

Case I: $r > r_A$

The strength of the magnetic interaction will be different for a planet inside or outside the Alfven radius of its host star. Let us first consider the case in which the distance between the planet and the star is larger than the Alfven radius. In this situation, the plasma transports the magnetic field lines from the star to the planet magnetosphere. Magnetic reconnection occurs on the surface of the magnetosphere, where the stellar wind pressure is balanced by the magnetic pressure of the planet. At this distance, the dominant component of the stellar wind velocity will be the radial component,

which we denote as V_w. As such, equation (2.14) becomes

$$P = V_w B_{MP}^2 R_{MP}^2 \text{ erg/s}. \tag{2.20}$$

Since V_w is large at a large enough distance from the star (i.e. $V_w > 200$km/s at $r = 0.1$ AU for the Sun), the power released will also be significant. As an example, the distance between the Sun and Jupiter is larger that the Alfven radius of the Sun, and so the magnetic reconnection between the solar and jovian magnetic fields takes place outside the Alfven radius, having a high intensity.

Case II: $r < r_A$

We now consider the case in which the distance between the planet and its host star is smaller than the Alfven radius, which is the case for most extrasolar planets detected so far. In this situation, the magnetic field lines of the planet and of the star are continuously connected. The plasma will flow along the magnetic field lines from the star to the planet. Since the magnetic field lines corotate with the plasma, the stellar wind velocity is now given by its tangential component, and it is a relative velocity [11]:

$$v_{rel} = K(R_*/A) - v_{rot}, \tag{2.21}$$

with K the orbital velocity and v_{rot} the equatorial rotational velocity of the star. Additionally, the continuous magnetic connection between the star and the planet will cause an enhanced, turbulent activity at the surface of the star, which will be characterized by a velocity $v_{mac}/\sqrt{2}$, the mean rms granular convective velocity at the stellar surface, observationally seen as rms macroturbulence. Therefore, the total tangential stellar wind velocity is [11]

$$V_\phi = (v_{mac}^2/2 + v_{rel}^2)^{1/2}, \tag{2.22}$$

and hence equation (2.14) becomes

$$P = V_\phi B_{MP}^2 R_{MP}^2. \tag{2.23}$$

However, v_{mac} is generally small ($v_{mac} \approx 0.5$km/s for the Sun [12]). Furthermore, as we will see in section 2.4, most extrasolar planets will become tidally locked to their host stars after a relatively short period of time. As such, the relative velocity v_{rel} will be very small, since it is expressed as the difference between the orbital velocity of the planet and the rotational velocity of the star, which will be equal in the case of tidal locking. The conclusion we draw is that the power released from magnetic reconnection will generally be weak inside the Alfven radius, and hence not easy to observe.

Another possibility of magnetic interaction between a planet and its host star inside the Alfven radius is an interaction similar to the one between Jupiter and its satellite Io. This type of interaction is believed to produce Alfvenic waves [43]. These waves produce electrical currents that accelerate the electrons in the plasma to energies of the order of keV, causing a significant energy release. The power dissipated in this situation can be expressed as [43]

$$P = \frac{M_a}{4(1+M_a^2)^{1/2}} B^2 v_{rel} R_{MP}^2, \tag{2.24}$$

where M_a is the Alfvenic Mach number and is approximately equal to 0.3 for the jovian magnetosphere.

Reconnection power dissipated

We now go back to making a qualitative estimate for the reconnection power from equation (2.14). The stellar wind velocity is generally difficult to estimate; however, the stellar wind model described in [29] predicts that the stellar wind velocity will not vary significantly for different types of stars. As such, we can estimate it to be constant and equal to the solar wind velocity at a distance equal to the distance be-

tween the star and the planet (for distances of the order ~ 0.05 AU, $V_w \approx 200$ km/s).

From [38] and [15], the magnetosphere radius can be expressed as a function of the planetary magnetic moment and the characteristics of the solar wind [1]:

$$R_{MP} = \left(\frac{\mu_0 f_0 M_D^2}{8\pi \rho_w V_w^2}\right)^{1/6}, \tag{2.25}$$

where M_D is the magnetic dipole moment of the planet (see equation (2.12)), ρ_w and V_w are the density and velocity of the stellar wind at the magnetosphere, A is the distance between the planet and the star, and f_0 is a form factor equal to $f_0 = 1.5$ for a spherical magnetosphere, but a more realistic estimate is $f_0 = 1.16$ [15]. In our calculations, we will assume f_0 has the same values for all planets. Assuming spherical symmetry, the density of the stellar wind at the radius of the planet is by definition

$$\rho_w = \frac{\dot{M}_*}{4\pi A^2 V_w}, \tag{2.26}$$

where $\dot{M}_*$ is the mass loss rate of the host star. From equations (2.25) and (2.26) we therefore obtain the following expression for the magnetosphere radius:

$$R_{MP} = \left(\frac{\mu_0 f_0^2}{2\pi}\right)^{1/6} M_D^{1/3} \dot{M}_*^{-1/6} V_w^{-1/6} A^{1/3}. \tag{2.27}$$

We can use observations to estimate the mass loss rate of the star [38], [42]:

$$\dot{M}_*[\dot{M}_\odot] = \left(\frac{R_*}{R_\odot}\right)^2 \left(\frac{F_X}{F_{X,\odot}}\right)^\delta, \tag{2.28}$$

where $\dot{M}_\odot$ is the mass loss rate of the Sun and (equal to $2 \times 10^{-14} M_\odot$/year), $F_{X,\odot}$ is the solar x-ray surface flux (equal to 31 $Jm^{-2}s^{-1}$) and $\delta = 1.15 \pm 0.20$. F_X is the X-ray flux at the surface of the star:

$$F_X = \frac{L_X}{4\pi R_*^2}, \tag{2.29}$$

[1]The expression for the magnetosphere radius is derived from the fact that the ram pressure of the stellar wind is equal to the magnetic pressure at the magnetosphere.

where L_X is the X-ray luminosity of the star, which is usually determined from observations. Once we know the value of the X-ray luminosity we can estimate the mass-loss rate of the star $\dot{M}_*$. In the next sections we will find empirical relations for L_X.

Next, we want to calculate the strength of the magnetic field B_{MP} at the magnetopause. From equation (2.12) (taking, for simplicity, $\theta = 0$), we obtain that

$$B_{MP} = \frac{M_D}{R_{MP}^3}. \tag{2.30}$$

But from equation (2.27), $R_{MP}^3 \propto M_D \dot{M_*}^{-1/2} V_w^{-1/2} A$. From this and equation (2.30) we obtain that the magnetic field strength at the magnetopause can be expressed as

$$B_{MP} \propto \dot{M_*}^{1/6} V_w^{1/6} A^{-1/3}. \tag{2.31}$$

We thus notice that in this model, the magnetic field strength at the magnetopause does not depend on the strength of the magnetic field at the surface of the planet, and can therefore be easily calculate with basic information about the host star parameters, and the distance between the star and the planet.

By substituting equations (2.27) and (2.31) into equation (2.14), we obtain that the power due to reconnection will be of the form

$$P \propto M_D^{2/3}. \tag{2.32}$$

Since the magnetic dipole moment of the planet can be expressed as $M_D = Br_0^3$, where B is given by equation (2.11), we finally obtain that the reconnection power will only depend on r_0, ρ_0 and λ - the dissipated power from reconnection scales as $\sim B^{2/3}$:

$$P \propto r_0^2 (\rho_0 \lambda)^{1/3}. \tag{2.33}$$

2.3.2 Power to mass relationship

In this section we relate the power dissipated through magnetic interaction between the planet and the star to the mass of the planet. From equation (2.33)

$$P \propto r_0^2 \rho_0^{1/3} = (\rho_0 r_0^3)^{1/3} r_0. \tag{2.34}$$

But $\rho_0 r_0^3$ represents a fraction f of the total mass of the planet M_P: $\rho_0 r_0^3 = f M_P \propto M_P$, and so we obtain that

$$P \propto M_P^{1/3} r_0. \tag{2.35}$$

2.3.3 A different model for the dissipated power

[11] makes a different estimate for the power of magnetic field interaction between a planet and its host star for the case of hot Jupiters. By analogy, we can derive an expression for the energy flux (power) due to magnetic interaction in the case of super Earths.

[11] derives the following expression for the dissipated power:

$$P \propto \frac{\epsilon B_* B^{1/3} v_c}{d^2 R_P^2 F_X^{1/6}}, \tag{2.36}$$

where ϵ is the fraction of total magnetic energy per unit time that magnetic interaction releases, B_* and B are the mean magnetic fields averaged over the surface of the star and planet, respectively, v_ϕ is the tangential component of the stellar wind velocity (see section 2.3.1), A is the distance between the star and the planet, R_P is the radius of the planet and F_X is the X-ray flux at the surface of the star. In the case of super Earths, the radius of the planet R_P is replaced by the radius of the core r_0:

$$P \propto \frac{\epsilon B_* B^{1/3} v_c}{d^2 r_0^2 F_X^{1/6}}. \tag{2.37}$$

It is further assumed in [11] that $B_* \propto P_{rot}^{-1.7}$, where P_{rot} is the period of rotation

of the star. The X-ray flux at the surface of the star F_X is related to the X-ray luminosity L_X observed on Earth by equation (2.29).

By contrast with the expression of dissipated power derived in section 2.3.1, the power derived by [11] scales as $\sim B^{1/3} r_0^{-2}$. By analogy to equation (2.35), $F_{int} \sim M_P^{1/6} r_0^{-5/2}$ in this case.

2.4 Tidal Locking

One factor that can affect the strength of the magnetic interaction between a planet and its host star is tidal locking. Tidal locking occurs when one (smaller) celestial body is forced to always face another (larger) celestial body, due to tidal forces. These forces arise due to the fact that the gravitational force exerted by the larger body upon the smaller body is not uniform: the side closer to the large body experiences a stronger force, while the other side experiences a weaker force. An example of tidal locking is the Earth-Moon system: one side of the Moon always faces the Earth, while the other never does. Tidal locking causes the 'locked' body to rotate around the other body in the same amount of time that it takes it to rotate around its own axis. This phenomenon is also called synchronous rotation. The time scale for a body to become tidally locked is given by [14]:

$$\tau_{sync} \approx Q\Big(\frac{R_P^3}{GM_P}\Big)(\omega_i - \omega_f)\Big(\frac{M_P}{M_*}\Big)^2\Big(\frac{A}{R_P}\Big)^6, \tag{2.38}$$

where Q is the planet tidal dissipation factor, R_P and M_P are the radius and mass of the planet, respectively, M_* is the mass of the hose star, ω_i and ω_f are the initial and final angular velocities of rotation, respectively (before and after tidal locking), G is the gravitational constant and A is the distance between the star and the planet. It is easy to notice that the synchronization time will be shorter for a smaller distance between the star and the planet. Since most discovered super Earths orbit very close to their host star, we expect these planets to become tidally locked to their host stars

after a relatively short period of time ($\tau_{sync} < 0.1$Gy [14]). After the tidal locking, the synchronous angular velocity of rotation (ω_f) will be given, from Kepler's law, by

$$\omega_f = \sqrt{\frac{M_* G}{A^3}}. \tag{2.39}$$

In section 2.3.1, we derived that the power resulting from magnetic reconnection is proportional to the strength of the magnetic field of the planet to a given power; the magnetic field, on the other hand, is $\sim \omega^{1/2}$ from equation (2.11). Since tidal locking causes the angular velocity of the planet to decrease, the magnetic field and hence the reconnection power will also have relatively small values compared to unlocked planets, and hence detection will be difficult.

2.5 Observations

In this section we discuss the different means by which power can be dissipated and observed in radio emissions, X-ray emissions and ultraviolet (UV) emissions. The dissipated total power derived in equation (2.14) can be written as

$$P = f_r P_r + f_x P_x + f_{uv} P_{uv}, \tag{2.40}$$

where P_r is the radio power, P_x is the X-ray luminosity, P_{uv} is the UV power, and f_r, f_x, f_{uv} are numbers between 0 and 1 representing the fractions of power that are emitted through radio, X-ray and UV, respectively.

2.5.1 Radio emission

The observation of radio emissions from extrasolar planets can be useful for several reasons. For example, it can provide another possible means of observing the planet directly and of finding information about its rotation period or its inclination. More importantly, the radio emission of a planet is related to the energy release at the magnetosphere (see section 2.3.1), so observations of radio emissions can give an estimate

of the planetary magnetic field. The magnetospheric radio emissions can have several origins: synchrotron radiation, thermal radiation or electron cyclotron maser radiation. The flux intensity of the different emissions is depicted in Fig. A-3 for various planets of the solar system. We notice that the strongest emissions are produced by the electron cyclotron maser radiation, so we will discuss this type of emission in more detail. This type of radiation is associated with planetary magnetic fields. In this process, electrons with energies of the order of 10^3 eV radiate power at a frequency equal to the gyrofrequency of the magnetic field lines. These emissions usually occur in regions of very low plasma density [16].

We follow again the derivations from [38] and adapt them to the case of super Earths. In radio emissions, the emitted power is observed as radio flux: the radio flux is measured in Jansky (symbol Jy), and 1 Jy=10^{-26}W/m^{2}Hz. We denote the radio flux emitted by the planet as P_r. Since different fractions of the solar wind kinetic flux (proportional to the ram pressure) and of the magnetic energy flux (proportional to the magnetic pressure) will be emitted through radio waves, we have the following relations:

$$P_r = \alpha P_{ram} = \beta P_{mag}, \tag{2.41}$$

where P_{ram} is the stellar wind kinetic flux, P_{mag} is the incident magnetic energy flux on the magnetosphere of the planet, and α and β are constants, also known as efficiency coefficients. From [38], P_{ram} is defined as

$$P_{ram} = \rho_w V_w^3 \pi R_{MP}^2, \tag{2.42}$$

(with ρ_w the stellar wind density at the magnetosphere). Using equation (2.26), P_{ram} can also be written as

$$P_{ram} = \frac{\dot{M}_* V_w^2 R_{MP}^2}{4A^2}. \tag{2.43}$$

From this and the expression for R_{MP} given in equation (2.27) we obtain that the

radio flux emitted by the planet will be given by

$$P_r \propto \dot{M_*}^{2/3} V_w^{5/3} B^{2/3} r_0^2 A^{-4/3}, \tag{2.44}$$

as calculated at the surface of the star. However, since we can only measure the radio emission from the Earth, we need an expression for the radio flux at the surface of the Earth. This will have an additional D^{-2} dependence, where D is the distance to the star:

$$P_r \propto \dot{M_*}^{2/3} V_w^{5/3} B^{2/3} r_0^2 A^{-4/3} D^{-2}. \tag{2.45}$$

For constant M_*, V_w, A and D, and using the dynamo magnetic field strength derived in equation (2.11), we obtain a scaling relation for P_r of the form:

$$P_r \propto r_0^2 (\rho_0 \lambda)^{1/3}, \tag{2.46}$$

where the proportionality constant can be determined from the known radio emission of Jupiter. We notice that this relation is consistent with the one derived in 2.33, which makes sense, as both scaling models have the same basic assumptions. We assume, based on equation (2.40), that the power resulting from each type of emission (X-ray, radio, UV) will be of the form $P_j \sim B^{2/3}$, where $j = r, x, v$.

2.5.2 Peak frequency for radio emission

In order for the radio flux to be detected through observations, we need to know the frequency for which the peak radio emission will occur. Following the derivations in [38], we first define two important frequencies - the plasma frequency denoted as ν_p, and the electron cyclotron frequency, denoted as ν_c. The plasma frequency represents the collective oscillation frequency of electrons in a plasma in the absence of a magnetic field. It is defined as

$$\nu_p = \left(\frac{n_e e^2}{\pi m_e}\right)^{1/2} = 8.98 \times 10^{-3} \text{ MHz}. \tag{2.47}$$

The electron cyclotron frequency represents the number of times per second that an electron orbits a magnetic field line, and is defined as

$$\nu_c = \left(\frac{eB}{2\pi m_e c}\right) = 2.8\left(\frac{B}{1Gauss}\right) \text{ MHz}, \tag{2.48}$$

where e is the electron charge, n_e is the electron density in cm^{-3}, and B is the magnetic field strength in Gauss at the surface of the conducting region of the planet (defined in equation (2.11)). [38] derives an empirical expression for the value of the frequency for which the radio emission is maximum: it is found that the magnetic field strength at the surface of Jupiter is $B \approx 4.3$ Gauss, corresponding to an electron cyclotron frequency of 12 MHz. This value is roughly equal to the observed frequency of the peak radio emissions from Jupiter. As such, it is approximated that peak emissions will occur at a frequency equal to the cyclotron frequency:

$$\nu_{peak} = \nu_c = 2.8B. \tag{2.49}$$

As such, the peak frequency will scale as:

$$\nu_{peak} \propto (\rho_0 \lambda)^{1/2}. \tag{2.50}$$

It is important to notice that observations of radio emission are only possible if the peak frequency is larger than the plasma frequency for the said star - radio waves with a lower frequency will always be screened, since radiation with frequency below the plasma frequency will always be trapped within the magnetosphere [28].

2.5.3 X-ray emission

As mentioned in section 2.5, a fraction of the reconnection power will be emitted through high energy X-rays from the stellar corona. These X-ray emissions are generally caused by thermal bremsstrahlung. As mentioned in section 2.3.1, the coronal activity is directly influenced by the magnetic interaction between the star and an orbiting planet. As such, the existence of a planet in the proximity of a star will

produce changes in the X-ray output, providing information with regards to the magnetic properties of the planet.

[35] finds an empirical relationship between the X-ray luminosity and the projected mass of hot Jupiters. This relation applies for distances between the star and the planet smaller than 0.15 AU, which is our domain of interest, since most super Earths have a distance to their host star less than 0.15 AU. He finds the following empirical relationship:

$$L_x = (3.58 \pm 0.01) \times 10^{28} (M_P \sin i)^{0.60 \pm 0.12} \text{ erg/s}, \tag{2.51}$$

where L_x is the sum of the time-averaged X-ray luminosities of the star and of the planet, and i is the inclination angle of the planet (the angle between the orbital plane and the ecliptic plane). Notice that the theoretical model presented earlier, $L_X \propto M_P^{0.33}$, (see equation (2.35)), is different from the empirical relation derived above. This might be caused by the fact that the model we are assuming is too simple. Additionally, choosing a different scaling model for the power dissipated (see, for example, [14]) might yield a theoretical result in agreement with observations.

2.5.4 UV emissions

A fraction of the energy resulting from magnetic reconnection will be emitted in the Ca II H & K lines. The Ca II & H lines are two absorption lines of singly-ionized calcium in the ultraviolet region of the spectrum, with wavelengths of 3968.5 $\mathring{A}$ and 3933.7 $\mathring{A}$, respectively [2]. The energy resulted from these emissions quantifies the amount of light emitted from the active magnetic regions of the stars. Since the stellar activity is influenced by the presence of an orbiting planet (see section 2.3.1), the emissions in the Ca II H & K lines will be significant when there is a strong magnetic interaction between the star and the planet. In particular, the prominence of the Ca II H & K lines can indicate a strong magnetic activity in the stellar chromosphere [2].

The Ca II H & K emissions have been studied for extrasolar giant planets. In [37], the

chromospheric activity in the Ca II H & K lines of several hot Jupiters is monitored over the course of several years (three years for most planets). The long exposure is necessary in order to obtain reliable information regarding the stellar activity and stellar cycles. [37] concludes that the stars with closely orbiting planets ('close-in' exoplanets) exhibit higher emissions in the Ca II H & K lines than the stars without planets. This indicates the existence of magnetic interactions between the planets and their host stars, as well as the fact that the energy released from these interactions can be detected through UV emissions. [37] quantifies the Ca II H & K emissions for several extrasolar planets, but does not provide a quantitative relationship between these emissions and the properties of the magnetic fields of the star and the planet. Currently, there are no studies regarding the possibility of UV emissions for super Earths.

Chapter 3

Applications to Known Super Earths and Results

In this chapter we apply the model developed in Chapter 2 to two known super Earths, CoRoT 7-b and GJ 1214 b. We discuss the detection potential of emissions from these planets, and generalize our results for other super Earths. We further consider special cases for detections, such as solar flares, or planets around Ap stars and M dwarfs.

For convenience, we write again the formulas we derived in Chapter 2 that will be used in the next sections:

$$B = \sqrt{2\Omega\mu_0\rho_0\lambda} \propto (\rho_0\lambda)^{1/2} \tag{3.1}$$

$$\nu_{peak} = 2.8B \propto (\rho_0\lambda)^{1/2} \tag{3.2}$$

$$P_r \propto r_0^2(\rho_0\lambda)^{1/3} \propto \nu_{peak}^{2/3} r_0^2. \tag{3.3}$$

$$\tag{3.4}$$

We notice that, if we know the orbital angular velocity Ω and we measure the peak frequency ν_{peak}, then we can find $\rho_0\lambda$ from equation (3.2). Furthermore, if we also measure the radio flux P_r, we can find r_0 from equation (3.3).

3.1 CoRoT 7-b

3.1.1 Discovery and physical parameters

The extra solar planet CoRoT 7-b was discovered by the French space mission CoRoT in early 2009, through the transit method (see Chapter 1). [25]. It is the first super Earth with a measured radius and mass, and the smallest yet exoplanet with a measured diameter. The physical parameters of CoRoT 7-b and its host star are summarized in Table B.1. CoRoT 7-b orbits around the parent star CoRoT-7 at a distance of only 4.27 stellar radii, or 0.017 AU [40], and with an orbital period of 0.854 days [40]. Its radius was derived to be $R = (1.68 \pm 0.09)R_{\oplus}$ [40], where $R_{\oplus}$ is the Earth radius. The mass of the planet was measured through the radial velocity method by the HARPS spectrograph [31]: $M_P = (4.8 \pm 0.8)M_{\oplus}$ [31], where $M_{\oplus}$ is the mass of the Earth. It therefore has an average density of 5.6 ± 1.3 g/cm^3 [31]. It has an age of about 1.2-1.3 Gy [40] and an equilibrium temperature of 1800-2600 Kelvin [40]. The inclination angle between the axis of the planet and the orbital plane was determined to be $i = (80.1 \pm 0.3)$ deg [25].

The planet orbits around the host star CoRoT-7. CoRoT-7 is a main sequence yellow dwarf star (type G9V) [25], similar to our Sun. It has a mass $M_* = (0.93 \pm 0.03)M_{\odot}$ [4] and a radius $R_* = (0.87 \pm 0.04)R_{\odot}$ [4]. CoRoT-7 is at a distance of 150 ± 20 parsecs [4] away from us (1 parsec= 3×10^{13} km) and it has a rotation period of 23 days [40].

3.1.2 Internal composition

Due to an average density similar to that of the Earth, CoRoT 7-b is believed to have a predominantly rocky structure [40]. In [40], several possible internal structures are presented, compatible with the known physical parameters of the planet. The first scenario is an iron-rock-ice planet, with an iron core, a silicate mantle and an ice layer. The second model is that of a steam planet, again with an iron core, a silicate

mantle and a (possibly H-He) layer of steam. The final possibility consider by [40] is an evaporated ice or gas giant. However, this last scenario is highly incompatible with the observed parameters of the planet. The conclusion reached by [40] is that CoRoT 7-b is most likely made of iron and silicates, which allow a mass range between 4 and 15 $M_{\oplus}$. The determined mass of the planet is therefore compatible with the rocky structure model.

3.1.3 Magnetic field strength

All possible compositions of CoRoT 7-b considered so far imply the existence of a molten core. As such, due to convection in the mantle, the planet is likely to generate a dynamo magnetic field, as described in section 2.1.1. Since the orbital period of CoRoT 7-b is $P = 0.854$ days (see section 3.1.1), we find $\Omega = 2\pi/P = 8.52 \times 10^{-5} s^{-1}$. We would first like to obtain a rough estimate of the magnetic field strength B. As such, we assume, for example, $\lambda \approx 2m^2/s$ for terrestrial planets [39]. We obtain approximate values for ρ_0 and r_0 by assuming an iron core mass fraction of 32 %, as approximated in [41]: $r_0 \approx 5400$ km and $\rho_0 \approx 15000$ kg/m^3. By plugging in these numbers into equation (2.11), we obtain a value for the intensity of the magnetic field B_0: $B_0 \approx 25$ Gauss, around 50 times bigger than that of the Earth ($B_{0,Earth} \approx 0.5$ Gauss). From equation (2.13), we obtain that the magnetic dipole moment is $M_D \approx 4 \times 10^{24}$ Am^2. Of course, the values of λ, ρ_0 and r_0 mentioned above are only true for a certain composition of the planet. Different internal compositions, however, will result in a different set of values for λ, ρ_0 and r_0.

3.1.4 Stellar X-ray emission

Currently, there is no precise data on the X-ray luminosity L_X of CoRoT-7. [25] sets an upper bound on the luminosity L_X of CoRoT-7: $L_X(CoRoT-7) < 5 \times 10^{28}$ erg/s. Another way to estimate L_X is by using the empirical relationship between X-ray luminosity and planetary mass from equation (2.51). We thus find $L_X \approx 2.9 \times 10^{27}$ erg/s, within the upper bound from above. We notice, however, that the X-ray

luminosity that we are extrapolating is actually the sum of the X-ray luminosity of the star and the X-ray luminosity of the planet. However, the planetary X-ray emission is usually much smaller than the stellar X-ray emission, so the result we obtain is fairly accurate.

3.1.5 Magnetospheric radio emission

In this section we estimate values for the radio flux and the frequency of the peak radio emission of CoRoT 7-b. We calculate these values based on different properties of the planet, all of which are reflected in the strength of the magnetic field B at the surface of the planetary core.

From equation (2.49) we determine how the peak frequency of radio emission for CoRoT 7-b depends on the density of the core ρ_0 and the magnetic diffusivity λ:

$$\nu_{peak} = 2.8B = 0.4(\rho_0\lambda)^{1/2} \text{ MHz}. \tag{3.5}$$

Next, we attempt to estimate the radio emission flux for CoRoT 7-b, as defined in equation (2.45). We first need to estimate the stellar mass loss rate of CoRoT-7, using equation (2.28). We use the value of the X-ray luminosity from section 3.1.4, $L_X \approx 2.9 \times 10^{27}$ erg/s, to estimate the mass loss rate of CoRoT 7-b: $\dot{M}_*[\dot{M}_\odot] = 1.8$. With this information, we can find the dependence of the radio flux emission on ρ_0, λ and r_0:

$$P_r \approx 6.4 \times 10^{-18} r_0^2(\rho_0\lambda^{1/3}) \text{ mJy}. \tag{3.6}$$

We would now like to see how exactly the peak frequency and the emitted radio flux will vary for different internal structures of the planet. For a terrestrial planet with an inner core composed of mostly iron, the magnetic diffusivity will typically have values between 1 and 10 m^2/s [26]. In subsection 3.1.3 we assumed the density of the core to be $\rho_0 \approx 15000$ kg/m^3. We will now assume that ρ_0 varies between 5000 and 25000 kg/m^3. We therefore plot ν_{peak} as a function of λ for varying ρ_0. The result

can be seen in Fig. A-4. We notice that the peak frequency has a range of values between 30 and 200 MHz.

Next, we study the dependence of the radio flux P_r on ν_{peak} and r_0. From equations (3.5) and (3.6) we obtain the following relation:

$$P_r = 1.2 \times 10^{-17} \nu_{peak}^{2/3} r_0^2 \text{ mJy}. \tag{3.7}$$

We plot P_r as a function of ν_{peak}, where ν_{peak} varies between 30 and 200 MHz (as obtained above), and we vary r_0 between $0.1R_P$ and $0.5R_P$, where R_P is the radius of CoRoT 7-b. The resulting plot is shown in Fig. A-5. We can see that the radio flux emitted varies between 3×10^{-4} and 0.01 mJy. We will see in later sections of this chapter that these values are very small and not detectable with present or near future instruments.

3.2 GJ 1214 b

3.2.1 Discovery and physical parameters

The extrasolar planet GJ 1214 b was discovered by the MEarth project in December 2009, also through the transit method [3]. It is the second super Earth with a measured radius and mass, after CoRoT 7-b. The physical parameters of GJ 1214 b and parent star GJ 1214 are labeled in Table B.1. It orbits around the parent star GJ 1214 at a distance of only 0.0143 AU [9] (even closer than CoRoT 7-b), and with an orbital period of 1.58 days [9]. Its radius was derived to be $R = (2.68 \pm 0.13)R_\oplus$ [9]. The mass of the planet was determined through the Doppler shift in its spectrum to be $M_P = (6.55 \pm 0.98)M_\oplus$ [9]. It thus has an average density of 1.87 $\pm$ 0.4 g/cm^3 [33] (smaller than the average density of CoRoT 7-b). Its equilibrium temperature was determined to be between 393 and 555 Kelvin [9], while the inclination angle between the axis of the planet and the orbital plane is $i = (88.62 \pm 0.28)$ deg [9].

The planet orbits around the host star GJ 1214. GJ 1214 is a main sequence red dwarf star (type M4.5) [4]. Its mass is $M_* = (0.157 \pm 0.019)M_\oplus$ [4], while its radius is $R_* = (0.211 \pm 0.0097 R_\oplus$ [4]. GJ 1214 b is at a distance of 13 parsecs [4] away from us, more than 10 times closer than CoRoT-7.

3.2.2 Internal composition

Current observations do not provide much information about the internal structure of the planet, and there is no evidence of the presence of water yet. However, [33] presents three different possible models for the compositions of the planet. The first model is that of a mini-Neptune, with an iron core, a silicate mantle, a layer of water and ice, and an envelope composed of hydrogen and helium. For such a composition, the gas layer can constitute at most 3.2%-6.8% of the planetary mass. If the planet has a Ganymede-like structure (with an iron:sillicates:water/ice layers in the mass ratio 3:22:75 [33]), then the gas envelope has to account for 0.01%-0.6% of the mass of the planet.

The second model assumes a water planet, with a predominantly icy interior surrounded by a gas envelope. In this case, the planet interior consists of an iron core, a silicate mantle and a water envelope.

The final possibility is that of a super Earth with a purely rocky interior and a substantial gas layer. Since the planet has a relatively low average density, it needs to have a gas layer in order to balance the high density of the rocky interior.

3.2.3 Magnetic field strength

All possible compositions of GJ 1214 b considered so far imply the existence of a molten core. As such, the planet is likely to generate a dynamo magnetic field, as described in section 2.1.1. For GJ 1214 b, we find Ω to be $4.6 \times 10^{-5} s^{-1}$. Same as for CoRoT 7-b, the magnetic field strength at the surface of the core will be a function

of the density of the core ρ_0 and the magnetic diffusivity λ (see equation (3.1)):

$$B = 0.1(\rho_0 \lambda)^{1/2}. \tag{3.8}$$

Similarly to the case of CoRoT 7-b, we first obtain a rough estimate of the magnetic field strength of GJ 1214 b at the surface of the core. We perform this calculation under the assumption that GJ 1214 b has a rocky structure. Currently there is no data on the possible radius of the core of GJ 1214 b. From [24], we estimate r_0 of GJ 1214 b to be $r_0 \approx 5900$ km. From [41], we estimate the density of the core to be $\rho_0 \approx 21000$ kg/m^3 [1]. We use the same values for the magnetic diffusivity of the planet as we used for CoRoT 7-b, $\lambda \approx 2m^2/\text{s}$. As such, we derive the magnetic field strength at the surface of the core to be $B \approx 20$ Gauss.

Magnetic field discussion

Before proceeding further, it is important to point out that a water/icy interior may produce a more complex magnetic field than the dipole assumption. In this situation, the magnetic field may have a quadrupole nature [24], with its strength decaying as $\sim r^{-4}$, as opposed to the dipole field that decays as $\sim r^{-3}$. In the solar system, the magnetic fields of Uranus and Neptune exhibit this behavior. Therefore, the model of the planet-star interaction presented in section 2.3.1 will change. Additionally, the quadrupole field might decays very fast, which might make it difficult to distinguish between different models for the planet interior. However, since in this thesis we are only concerned about producing some qualitative estimates of the planet-star interaction and planetary emissions, we will assume that the magnetic field can still be represented as a dipole for an icy planet. We leave the more complex model open for future work.

[1] Under the assumption that the core constitutes 32% of the mass of the planet.

3.2.4 Stellar X-ray emission

There is currently no data on the X-ray luminosity of GJ 1214. Therefore, we use instead the average value for X-ray luminosity for M dwarfs. [8] finds this average value to be $2.3(+1.3, -1.4) \times 10^{28}$ erg/s. We will thus use $L_X \approx 10^{28}$ erg/s.

3.2.5 Magnetospheric radio emission

In this section we estimate values for the radio flux and the frequency of the peak radio emission of GJ 1214 b. Similar to the case of CoRoT 7-b, we calculate these values based on different properties of the planet, all of which are reflected in the strength of the magnetic field B at the surface of the planetary core.

From equation (2.49) we determine how the peak frequency of radio emission for GJ 1214 b depends on the density of the core ρ_0 and the magnetic diffusivity λ:

$$\nu_{peak} = 2.8B = 0.3(\rho_0\lambda)^{1/2} \text{ MHz}. \tag{3.9}$$

We then proceed to estimate the radio emission flux for GJ 1214 b, as defined in equation (2.45). We first need to estimate the stellar mass loss rate of GJ 1214 b, using equation (2.28). We use $L_X = 10^{28}$ erg/s and obtain $\dot{M}_*[\dot{M}_\odot] = 10.8$. With this information, we can find the dependence of the radio flux emission on ρ_0, λ and r_0:

$$P_r \approx 3.8 \times 10^{-12} r_0^2 (\rho_0\lambda)^{1/3} \text{ mJy}. \tag{3.10}$$

We are now interested to know how the peak frequency and radio emission will vary for different internal structures of the planet, as well as whether these emissions are detectable or not. Since the planet could have both a rocky or an ice predominant composition, we assume a larger range of magnetic diffusivities λ between 1 and 100 m^2/s, where the higher diffusivities correspond to the icy composition [39]. Moreover, since the average density of the planet is smaller than the average density of CoRoT 7-b, we will assume a range of smaller values for the core density ρ_0, between 10^3 and

10^4 kg/m^3. We plot ν_{peak} as a function of λ for varying ρ_0. The result can be seen in Fig. A-6. We notice that the peak frequency has a range of values between 10 and 300 MHz.

We now study the dependence of the radio flux P_r on ν_{peak} and r_0. From equations (3.5) and (3.10) we obtain the following:

$$P_r = 8.4 \times 10^{-12} \nu_{peak}^{2/3} r_0^2 \text{ mJy}. \tag{3.11}$$

We plot P_r as a function of ν_{peak}, where ν_{peak} varies between 10 and 300 MHz (as obtained above), and we vary r_0 between $0.1R_P$ and $0.5R_P$, where R_P is the radius of GJ 1214 b. The resulting plot is shown in Fig. A-7. We notice that the range of plausible radio flux emitted by GJ 1214 b varies roughly between 25 and 25000 mJy, which is several orders of magnitude larger that the radio flux emitted by CoRoT 7-b. This can be explained by the fact that GJ 1214 b is more than ten times closer to the Earth than CoRoT 7-b, thus producing a much stronger signal at the surface of the Earth. Additionally, host star GJ 1214 is an M-dwarf and hence has a higher activity than CoRoT-7, which results in a stronger X-ray emission. In contrast with CoRoT 7-b, we will see later in this chapter that the values obtained above for the peak frequency and the radio flux can be detectable with current instruments.

3.3 Detection potential

In this section we discuss the possibility of detection of radio, X-ray and UV emissions from super Earths with current instruments, as well as the potential for future detections. We first relate the results obtained in the previous sections for CoRoT 7-b and GJ 1214 b to observations and explain the detection potential of each planet. We then generalize our results for other super Earths.

3.3.1 Condition for dynamo existence

We first want to investigate under which conditions a dynamo magnetic field can exist (and hence when can magnetic interaction occur). In section 2.1.1, we obtained an expression for the magnetic field decay time after the dynamo stops:

$$\tau \sim \frac{r_0^2}{\pi^2 \lambda}. \tag{3.12}$$

Since we do not have any information regarding the dynamo decay time for exoplanets, we will use the known value for the Earth dynamo: $\tau \approx 10^4$ years. Using this, we obtain a relationship between the radius of the metallic region r_0 and the magnetic diffusivity λ that is depicted in Fig. A-8 and A-9. The first figure shows the allowed and forbidden dynamo regions for terrestrial planets, while the second figure shows the same regions for icy planets. The gray region in both figures represents the forbidden region, the region in which the dynamo decays very fast. We notice that our choice of parameters for CoRoT 7-b (see section 3.1) allows the existence of the dynamo, imposing however a lower bound for the radius of the core r_0: from the graph, r_0 needs to be larger than (roughly) 1000 km for the dynamo to be possible, which explains the lower bound that we chose for r_0 in Fig. A-5, $r_{0,min} = 0.1R_P \approx 10700$ km.

Similarly, if we consider GJ 1214 b to have a rocky composition, the dynamo will be possible for our choice of parameters, as can be deduced from Fig. A-10. If, however, we assume GJ 1214 b to have a predominantly icy interior, then different conductivities of the core will result in different lower bounds for the radius of the core r_0 in order for the dynamo to exist. For example, if $\sigma = 5 \times 10^3$ S/m, we obtain $r_{0,min} \approx 4000$ km $\approx 0.23R_P$.

3.3.2 Radio emission observations

In this section we discuss several current and future instruments for detecting radio emissions.

Giant Metrewave Radio Telescope (GMRT)

The GMRT is the world largest set of radio-wavelength telescopes [6] and is located in India. It was built in 1995 and it consists of 30 telescopes, with a collection area of 60750 km^2 [6]. It can detect radio waves with frequencies around 150 MHz, for a power limit of around 1 mJy [23].

Very Large Array (VLA)

The VLA is a radio astronomy observatory located in New Mexico. It consists of 27 independent antennas, each with a diameter of 25 meters [1]. The lowest radio frequency that it can detect is around 74 MHz at a resolution of 24 arcseconds [1]. The corresponding minimum power output is 135-300 mJy [23].

The Ukrainian T-shaped Radio Telescope, second modification (UTR-2)

UTR-2 is the world largest radio telescope at decameter wavelengths. It is located near Kharkiv, Ukraine and has a collective area of 15000 km^2. It detects frequencies between 8 and 40 MHz, with a sensitivity of 1000 mJy [23].

3.3.3 LOw Frequency ARray for radio astronomy (LOFAR)

LOFAR is a project of building an interferometric array of radio telescopes distributed across the Netherlands, Germany, Great Britain, France, Sweden and possibly other European countries. The total effective collecting area is aimed to be up to 1 km^2. LOFAR aims to detect frequencies between 10 and 240 MHz, with a resolution at 240 MHz better than one arcsecond and sensitivity of around 0.1 mJy or less. The first LOFAR station opened in November 2007 in Germany. Twenty additional LOFAR stations are currently being funded and constructed.

The detection potential of the above mentioned telescopes is depicted in Fig. A-10

and A-11 for CoRoT 7-b and GJ 1214 b, respectively. We notice that none of the telescopes can detect the very low signals emitted by CoRoT 7-b, which confirms our statement from section 3.1. On the other hand, we can easily see that the four telescopes cover the whole range of possible radio emissions from GJ 1214 b, which is an important result.

3.4 Special cases for detection

In this section we discuss some special situations in which the interaction between an extrasolar planet and its host star might be strong enough to be detected. We discuss solar flares and coronal mass ejections of M dwarfs, as well as their implications upon the habitability of exoplanets. We then briefly mention Ap stars.

3.4.1 M dwarfs: flares and coronal mass ejections

A stellar flare is a sudden explosion in the atmosphere of a star that releases a very large amount of energy. Flares are caused by magnetic reconnection (see section 2.3.1) and emit radiation in the entire electromagnetic spectrum: radio emissions, visible emissions, X-rays and gamma rays. Stellar flares can have a significant effect on the atmosphere and habitability of the orbiting planets. However, since stellar flares are irregular phenomena, occurring at fixed points in time and having a relatively short duration, they often have a very low statistical chance of detection [20]. Since there is strong evidence that M-dwarfs undergo frequent and strong flare-like events, detection of such events around M-dwarfs is more probable then around G-stars like our own Sun. If a stellar flare is extremely powerful, it can produce a coronal mass ejection (CME): ejection of plasma from the stellar corona. Flares and CMEs are therefore a manifestation of the same physical phenomenon, and so it can be expected that frequent stellar flares on M-dwarfs are associated with CMEs. [20] assumes that the CMEs from M-dwarfs are very similar in nature and in strength to solar CMEs, due to the fact that they are produced by the same basic mechanisms in similar coronal plasma conditions. Therefore, [20] models the CMEs from M-dwarfs based on the

known information regarding CMEs from the Sun. The study concludes that close-in exoplanets should experience a continuous CME exposure over long periods of time [20], which has strong implications upon the atmosphere and hence the habitability of such exoplanets.

The existence of stellar flares and CMEs can have important implications on the power dissipated due to magnetic reconnection. In particular, the stellar wind velocity V_w will increase significantly when such an event is produced. This, in turn, will increase the power dissipated due to magnetic reconnection defined in equation (2.14). Therefore, the radio emissions from the planet will also be stronger (with energies $> 10^{32}$ erg [20]), which increases the likelihood that these emissions will be observed. It is important to note, however, that such events are rare, and so the probability of detecting them is low.

3.4.2 Ap stars

Another possibly interesting set of stars to host extrasolar planets are the Ap stars. The 'Magnetic peculiar A' stars, commonly referred to as Ap stars, represent a small fraction of the main sequence A stars and are characterized by overabundance of some rare elements in their atmosphere, such as strontium, chromium and europium [21]. An important feature of the Ap stars is the fact that they produce strong magnetic fields, in the range of few hundred to 30000 Gauss [21]. So far there are no reported discoveries of exoplanets around Ap stars. However, the strong magnetic field of an Ap star suggests that, if a planet were to orbit such a star, the magnetic interaction between the star and the planet will be significant, and hence detectable. We leave this as a potential topic for future work.

Chapter 4

Discussion and Conclusions

In this thesis, we began by collecting and presenting various existing models of the magnetic field and the planet-star magnetic interaction between a giant extrasolar planet and its host star. We then adapted these models for the case of super Earths, specifically to two known planets. We summarize our results and findings in the next paragraphs.

First, we modeled the planetary magnetic field as a dynamo. We then presented a model of the magnetic interaction between a super Earth and its host star (section 2.1.1). We found that the mechanisms governing this interaction differ as a function of the distance between the planet and its host star. The interaction (mainly due to magnetic reconnection) will be stronger when the planet lies outside the Alfven radius of the star, and weaker inside the Alfven radius (section 2.3.1). We further assumed that the total energy released due to magnetic reconnection will be emitted only in the radio, X-ray and ultraviolet (UV) ranges of the electromagnetic spectrum (section 2.5). Based on existing models, we estimated the radio flux emitted by a super Earth and the frequency at which this emission is maximum as a function of the strength of the magnetic field at the surface of the planet (sections 2.5.1 and 2.5.2). Since this magnetic field depends on the internal composition of the planet (more precisely, on the radius, density and electrical conductivity of the planetary core), we were able to find a direct relation between the radio flux, peak frequency and some of the internal

physical parameters of the planet.

We estimated the frequency of peak emission and the strength of the radio flux for two recently discovered super Earths, CoRoT 7-b and GJ 1214 b (see Chapter 3). We considered several possible compositions for both planets (rocky, ice+rock mixture, water) (sections 3.1, 3.2). We first related the frequency of peak radio emission to the density and the electrical conductivity of the planetary core (equations (3.1-3.2)). Since both the peak frequency and the radio flux have similar dependences on the density and electrical conductivity of the core, we were able to eliminate the latter quantities and obtain an expression of the radio flux only as a function of the frequency of peak emission and the core radius (equation (3.3)).

Next, we compared the estimated emissions from CoRoT 7-b and GJ 1214 b with the detectability range of current and future instruments (section 3.3). We found that radio emission from CoRoT 7-b is very low, mainly due to a large distance between the Earth and the planet-star system (Fig. A-10). On the other hand, we found that the flux observed on Earth from GJ 1214 b is much stronger, mostly due to the fact that the planet is more than ten times closer to Earth than CoRoT 7-b. As such, the whole range of possible peak frequencies and radio fluxes can be detected with current instruments or instruments that will be functional shortly (Fig. A-11).

Lastly, we discussed briefly the possibility of detection around special types of stars, such as M-dwarfs and Ap stars (section 3.4).

The measurement and detection of the power released due to the magnetic interaction between an extrasolar planet and its host star can reveal important information regarding the internal composition of the planet. In the case of GJ 1214 b, for example, if we detect its radio emission in a small frequency range and subsequently a small radio flux range, we can find an estimate of the planetary core radius, as well as a relationship between the density and electrical conductivity of the core. This can

help us determine the composition of the planetary core. As we saw in Fig. A-11, the detection of GJ 1214 b emission in a certain frequency and flux range can help us distinguish between a rocky composition and an ice-dominated interior. Our calculations can be generalized for other super Earths; if emission from a super Earth is detected, important information regarding the internal structure of the planet can be revealed. Knowing the internal composition of the planet, as well as the activity of its host star (i.e. stellar flares or CMEs), can be vital in determining if the planet has the potential to be habitable or not, which is one of the main questions that planetary science is aiming to answer nowadays.

4.1 Directions for future work

This thesis aims to present a general model of the interaction between an exoplanet and its parent star. It can therefore serve as a starting point for more detailed studies of the magnetic fields of super Earths. For instance, the planetary magnetic field becomes more complex if we also take into account magnetic induction in the outer layers of the planet (which we are neglecting in this paper, see section 2.1.1). Another further development would be the more detailed modeling of the magnetic field in the case of a water/ice planet, taking into account its possibly quadrupolar nature (see section 3.2). Determining the internal composition of super Earths is a key topic in planetary science, since it directly affects the existence and composition of a planetary atmosphere (see, for example, [33]). It can also provide insight into the presence of liquid water and finally the possibility of the planet being habitable. Consequently, the study of the magnetic fields of super Earths and of the interaction between super Earths and their host stars can lead us to significant discoveries regarding the plethora of planets outside the solar system, and may help us to finally answer the perpetual question 'Does life on other planets exist?'.

Appendix A

Figures

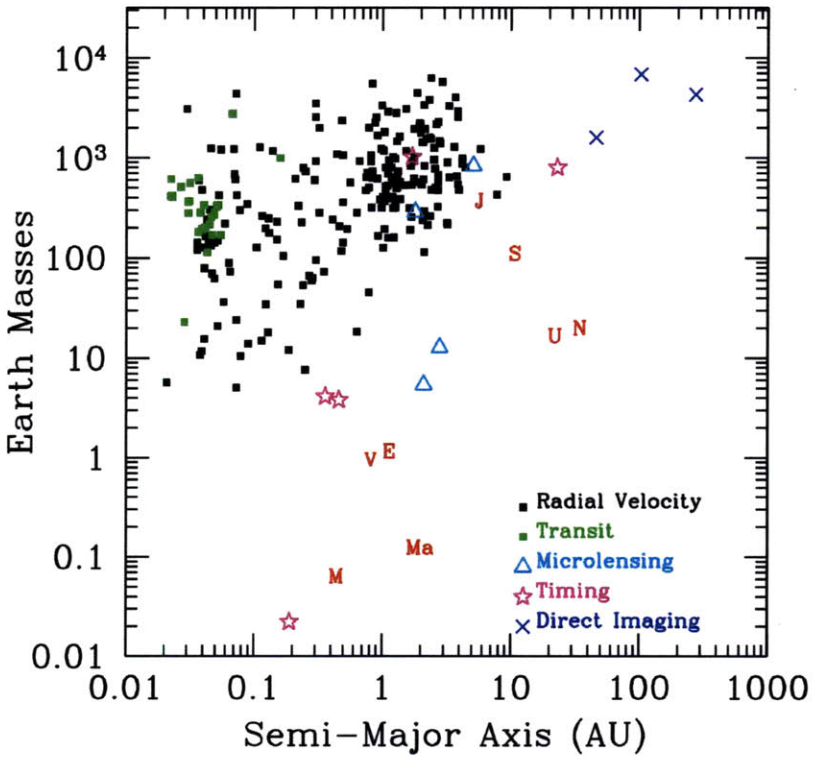

Figure A-1: Currently discovered exoplanets: mass versus radius diagram (Credit: Sara Seager)

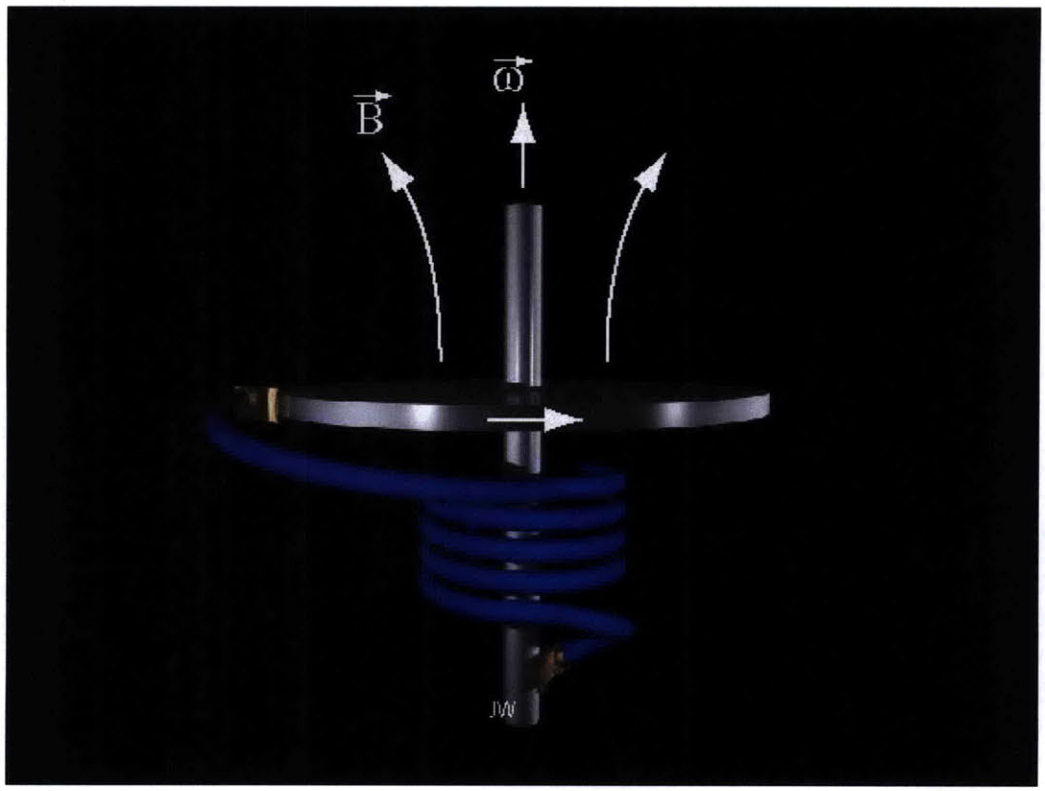

Figure A-2: The disc dynamo illustrates the principles of the dynamo process (Source: [36]). The rotation of an electrically conducting disc through a magnetic field induces electrical currents in the disc, which can themselves create B when guided through a coil.

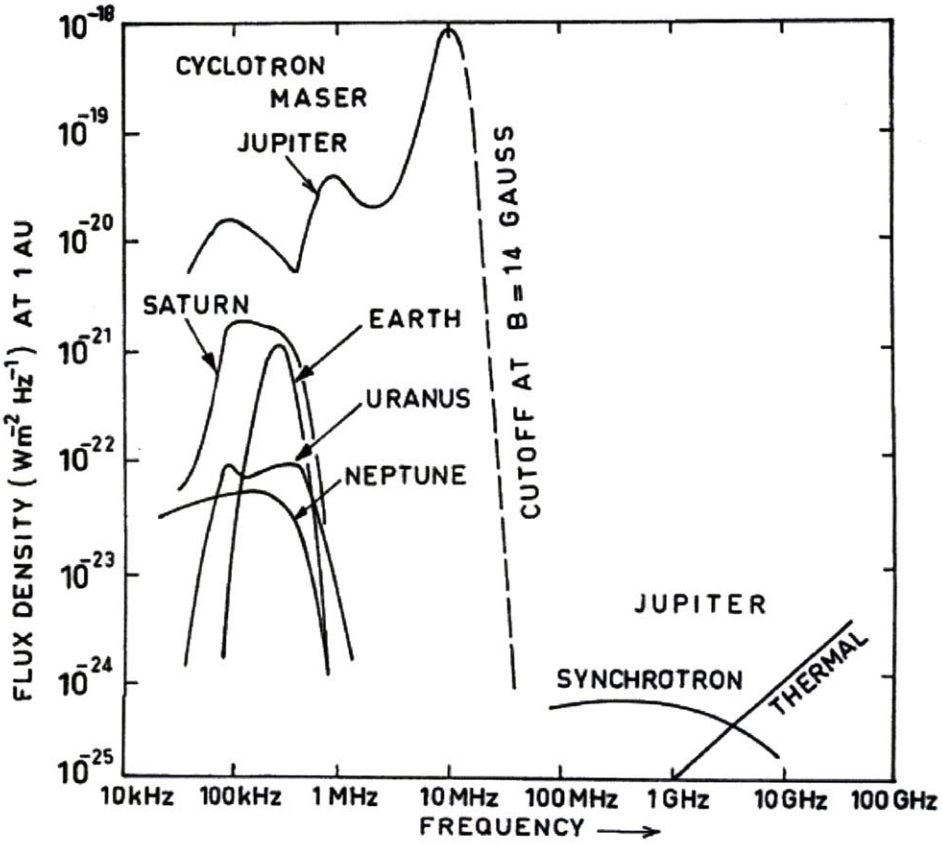

Figure A-3: Flux densities of solar system planets normalized to a standard distance of 1 AU (Source: [7])

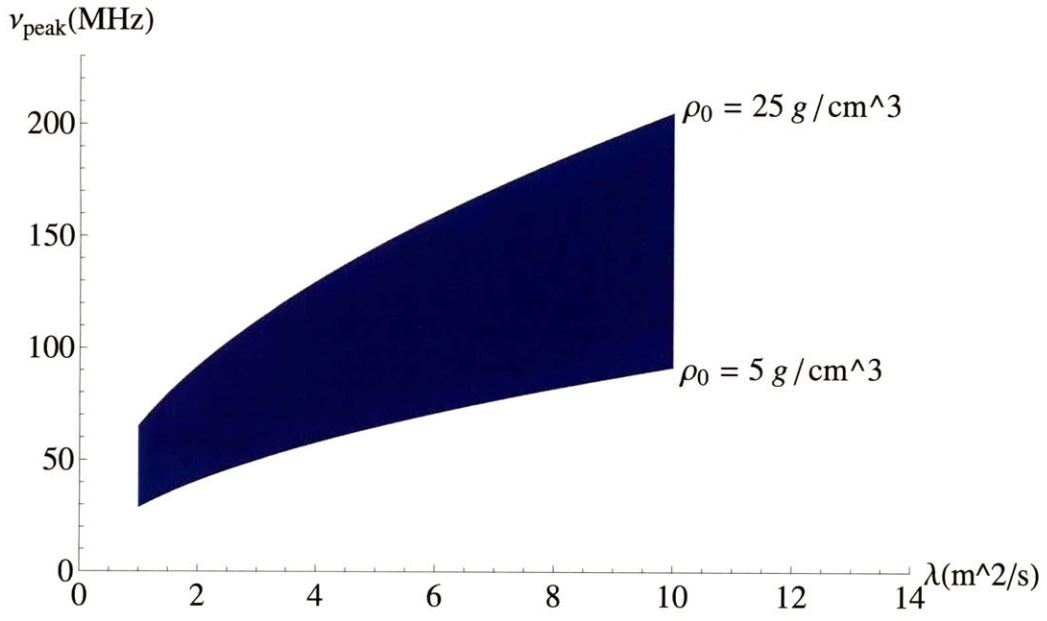

Figure A-4: CoRoT 7-b: ν_{peak} for varying λ and ρ_0

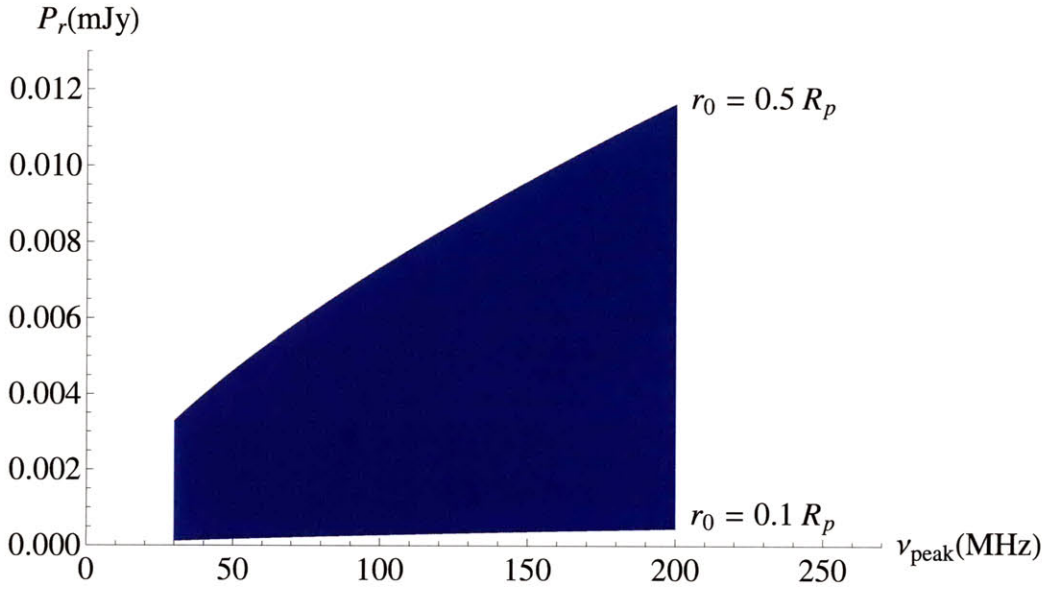

Figure A-5: CoRoT 7-b: P_r for varying ν_{peak} and r_0

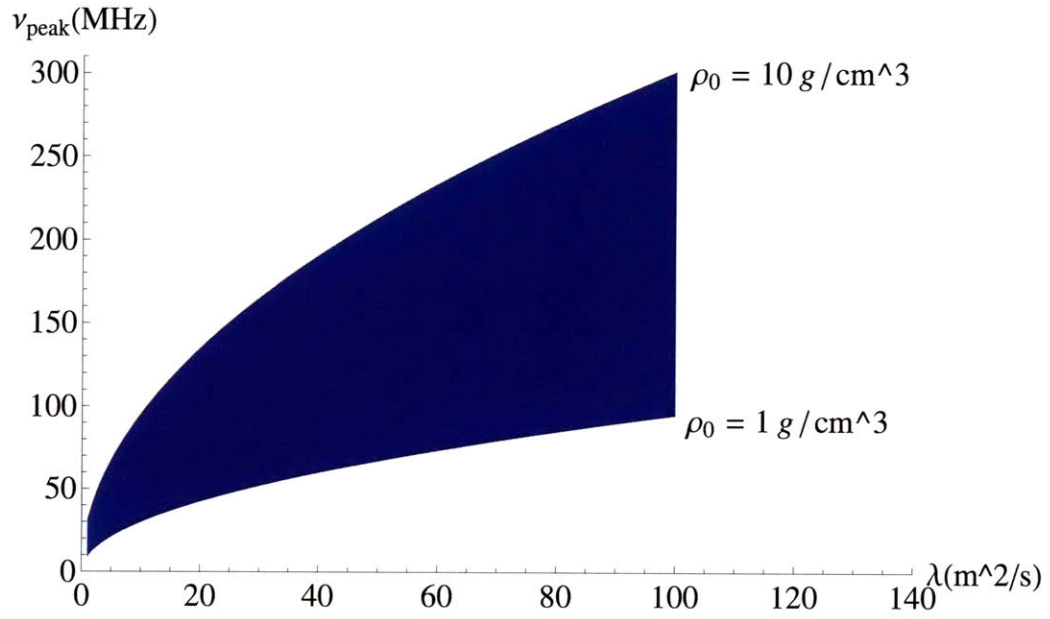

Figure A-6: GJ 1214 b: ν_{peak} for varying λ and ρ_0

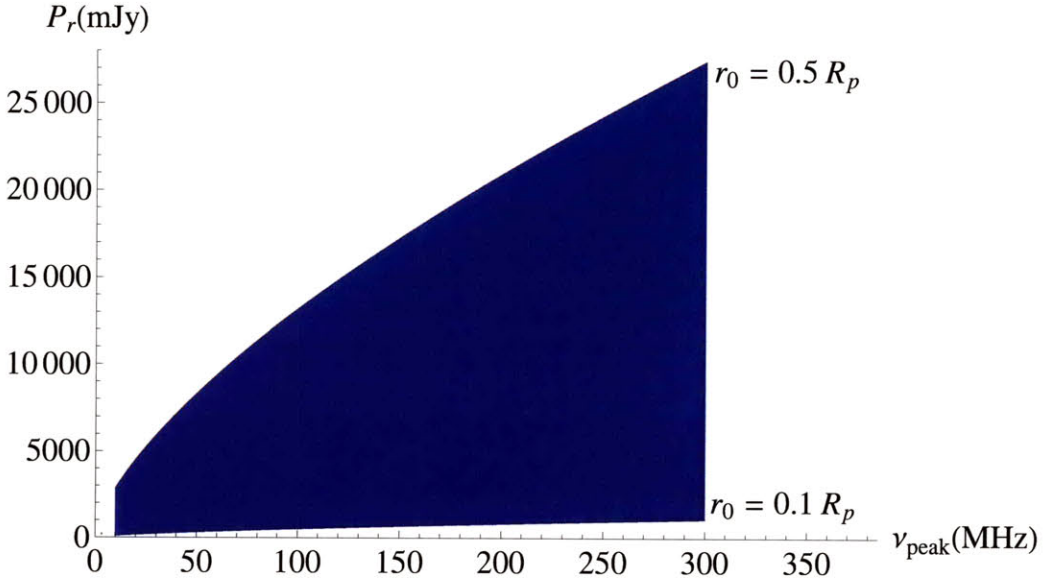

Figure A-7: GJ 1214 b: P_r for varying ν_{peak} and r_0

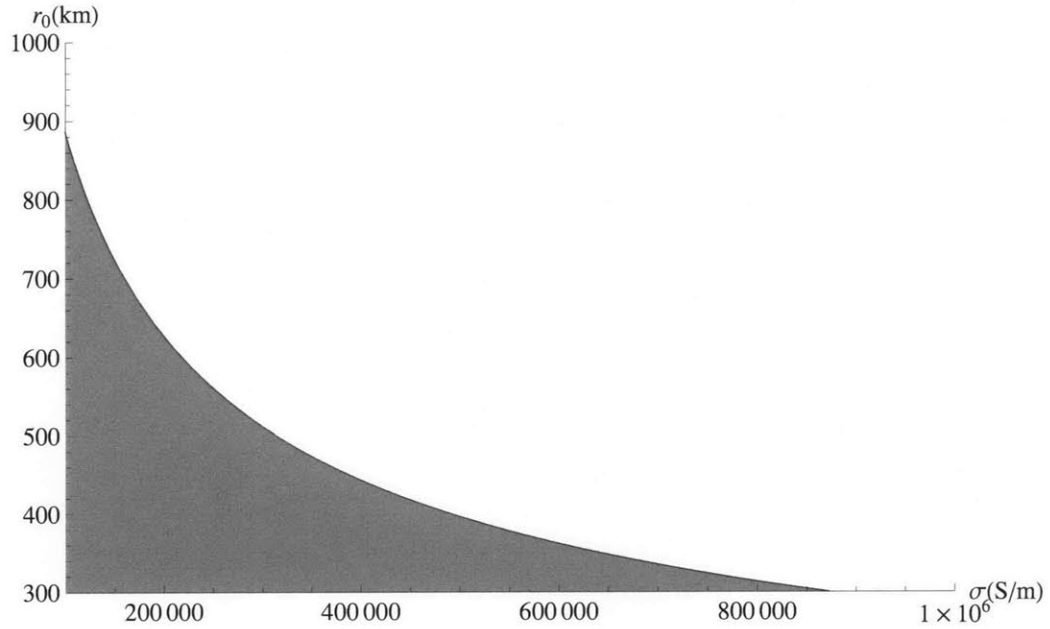

Figure A-8: Terrestrial planets: the allowed and forbidden region for a planetary dynamo to exist. The gray region represents the region in which the dynamo decays too fast

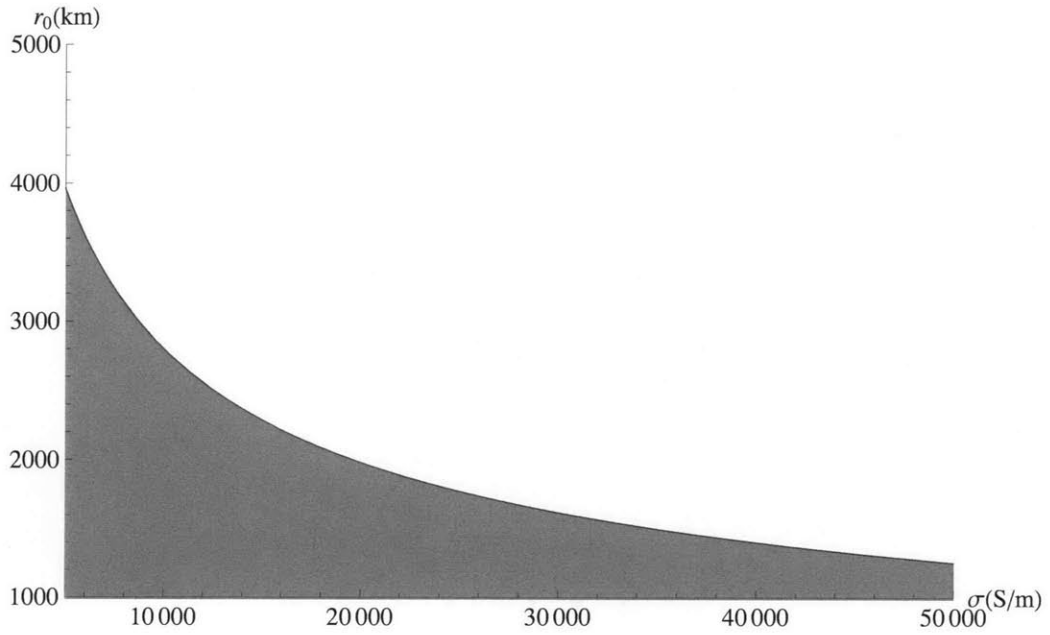

Figure A-9: Ice planets: the allowed and forbidden region for a planetary dynamo to exist. The gray region represents the region in which the dynamo decays too fast

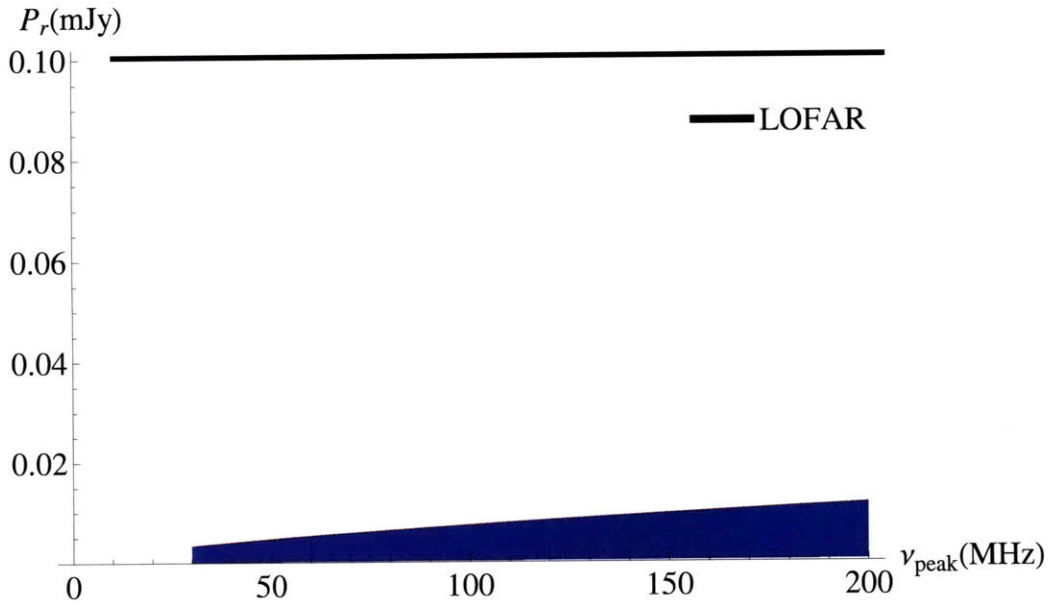

Figure A-10: Comparison between CoRoT 7-b predicted radio emissions and the range of sensitivities of several current and future instruments: detections are unlikely to be possible.

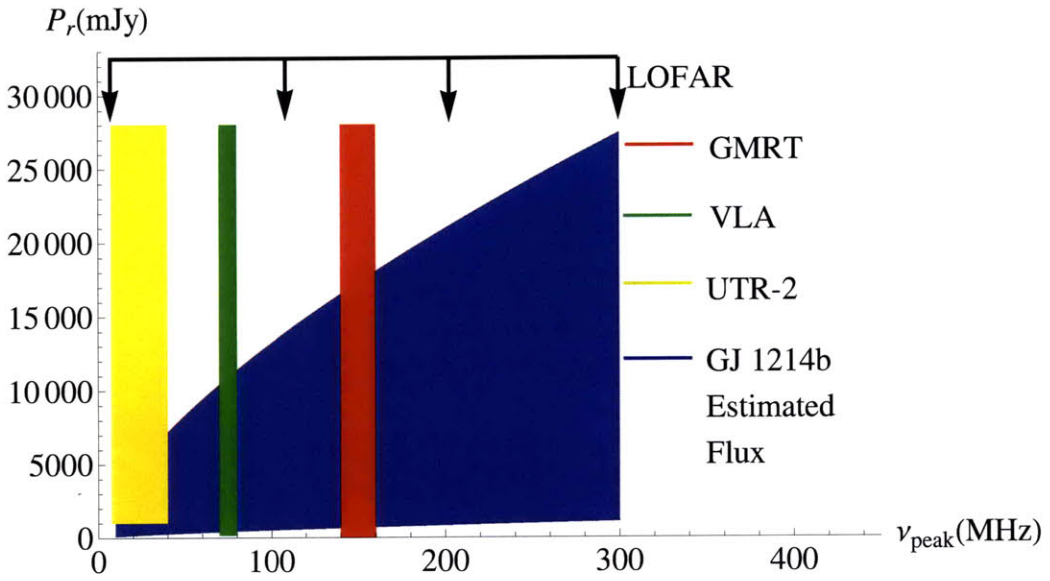

Figure A-11: Comparison between GJ 1214 b predicted radio emissions and the range of sensitivities of several current and future instruments: detections may be possible.

Appendix B

Tables

Table B.1: Physical parameters for CoRoT 7-b, GJ 1214 b and their and host stars

	CoRoT 7-b	GJ 1214 b
Radius (R)	$(1.68 \pm 0.09) R_{\oplus}$	$(2.68 \pm 0.13) R_{\oplus}$
Orbital period (P)	0.854 days	1.58 days
Distance to its host star (A)	0.017 AU	0.014 AU
Age	1.2-1.3 Gy	-
Equilibrium temperature (T)	$1800 - 2600$ K	$393 - 555$ K
Mass (M)	$(4.8 \pm 0.8) M_{\oplus}$	$(6.55 \pm 0.98) M_{\oplus}$
Average density (ρ)	(5.6 ± 1.3)g/cm^3	(1.87 ± 0.4)g/cm^3
Inclination angle (i)	(80.1 ± 0.3) deg	(88.62 ± 0.28) deg
P_{rot} of host star	23 days	-
Radius of star (R_*)	$(0.87 \pm 0.04) R_{\odot}$	$(0.211 \pm 0.0097) R_{\odot}$
Distance of star (D)	(150 ± 20) pc	13 pc
Mass of star (M_*)	$(0.93 \pm 0.03) M_{\odot}$	$(0.157 \pm 0.019) M_{\odot}$

Bibliography

[1] NRAO VLA. Official website ¡http://www.vla.nrao.edu¿.

[2] H and K lines. A Dictionary of Astronomy. 1997. Retrieved April 19, 2010.

[3] MEarth: looking for transiting, habitable super-Earths around small stars. 2009. Retrieved 2010-04-15.

[4] The Extrasolar Planet Encyclopaedia. Established in February 1995. Retrieved on 04-15-2010.

[5] Successful launch of the COROT satellite, on 27 December 2006. *Corot 2006 Events. CNES. 2007-05-24*, Retrieved 2010-04-15.

[6] S Ananthakrishnan. The Giant Metrewave Radio Telescope. *Journal of Astrophys. and Astron.*, 16:427–435, 1997.

[7] T. S. Bastian, G. A. Dulk, and Y. Leblanc. A Search for Radio Emission from Extrasolar Planets. *Astrophys. J.*, 545:1058–1063, 2000.

[8] J.-P. Caillault, D. J. Helfand, J. A. Nousek, and L. O. Takalo. X-ray-selected M dwarfs and the diffuse X-ray background. *Astrophys. Journal*, 304:318–325.

[9] David Charbonneau et al. A super-Earth transiting a nearby low-mass star. 2009.

[10] Andrew Cumming et al. The Keck Planet Search: Detectability and the Minimum Mass and Orbital Period Distribution of Extrasolar Planets. 2008.

[11] Manfred Cuntz, Steven Saar, and Zdzislaw Musielak. On stellar activity enhancement due to interactions with extrasolar giant planets. *Astrophys. Journal*, 533, 2000.

[12] G. H. E. Elste. The Distinction Between Micro- and Macroturbulence in the Solar Photosphere Using Line Profiles. *Astrophys. Journal*, 148, 1967.

[13] J.M. Griessmeier, U. Motschmann, G. Mann, and H. O. Rucker. The influence of stellar wind conditions on the detectability of planetary radio emissions. *Astron. and Astrophys.*, 437:717–726.

[14] J.M. Griessmeier, A. Stadelmann, U. Motschmann, N.K. Belisheva, H. Lammer, and H.K. Biernat. Cosmic Ray Impact on Extrasolar Earth-Like Planets in Close-in Habitable Zones. *Astrobiology*, 5, 2005.

[15] J.M. Griessmeier, A. Stadelmann, T. Penz, H. Lammer, F. Selsis, I. Ribas, E. F. Guinan, U. Motschmann, H. K. Biernat, and W. W. Weiss. The effect of tidal locking on the magnetospheric and atmospheric evolution of 'Hot Jupiters'. *Astron. and Astrophys.*, 425:753–762.

[16] Gurnett, D. A. *Planetary Radio Emissions. Astronomy and Astrophysics Encyclopedia.* 1992.

[17] http://kepler.nasa.gov/.

[18] http://sunearth.gsfc.nasa.gov.

[19] Wing-Huen Ip, Andreas Kopp, and Juei-Hwa Hu. On the star-magnetosphere interaction of close-in exoplanets. *Astrophys. Journal*, 602, 2003.

[20] Maxim L. Khodachenko, Ignasi Ribas, Helmut Lammer, Jean-Mathias Griemeier, Martin Leitner, Franck Selsis, Carlos Eiroa, Arnold Hanslmeier, Helfried K. Biernat, Charles J. Farrugia, and Helmut O. Rucker. Coronal Mass Ejection (CME) Activity of Low Mass M Stars as An Important Factor for The

Habitability of Terrestrial Exoplanets. I. CME Impact on Expected Magnetospheres of Earth-Like Exoplanets in Close-In Habitable Zones. *Astrobiology*, 7:167–184.

[21] J. D. Landstreet et al. Searching for links between magnetic fields and stellar evolution. II. The evolution of magnetic fields as revealed by observations of Ap stars in open clusters and associations. 2007.

[22] A. F. Lanza. Stellar coronal magnetic fields and star-planet interaction. 2009.

[23] J. Lazio et al. Magnetospheric Emission from Extrasolar Planets. 2009.

[24] K.K.M. et al. Lee. Laser-driven shock experiments on precompressed water: Implications for 'icy' giant planets. *J. Chem. Phys.*, 1255, 2006.

[25] A. Leger et al. Transiting exoplanets from the CoRoT space mission VIII. CoRoT-7b: the first Super-Earth with measured radius. 2009.

[26] E. H. Levy. Generation of planetary magnetic fields. *Annu. Rev. Earth Planet. Sci.*, 4:159–185, 1976.

[27] Longair, M. S. *High energy astrophysics: Stars, the Galaxy and the interstellar medium.* Cambridge University Press, Cambridge, 1994.

[28] McFadden, L. and Weissman, P. and Johnson, T. *Encyclopedia of the Solar System, Second Edition.* Academic Press, 2007.

[29] S. Preusse, A. Kopp, J. Buchner, and U. Motschmann. Stellar wind regimes of close-in extrasolar planets. *Astron. Astrophys.*, 434:1191–1200, 2004.

[30] S.B. Qian, Z.B. Dai, L.Y. Zhu, L. Liu, J.J. He, W.P. Liao, and L.J. Li. Magnetic Braking and the Evolution of the Hw Vir-like Binary Stars. *Astrophys. Journal*, 689, 2008.

[31] D. Queloz. The CoRoT-7 planetary system: two orbiting super-Earths. *Astron. Astrophys.*, 506:1, 2009.

[32] Paul H. Roberts and Gary A. Glatzmaier. Geodynamo theory and simulations. *Rev. Mod. Phys.*, 72:1081–1123, 2000.

[33] L. A. Rogers and S. Seager. Three Possible Origins for the Gas Layer on GJ 1214b. 2009.

[34] Sachdev, P. L. and Venkatachalappa, M. *Recent Advances in Fluid Mechanics.* Gordon and Breach Science Publishers, Amsterdam, 1998.

[35] Caleb A. Scharf. Possible constraints on relative exoplanet magnetic field from planet-star interaction. draft of paper sent to the authors, March 3 2010.

[36] Schubert, Gerald. *Treatise on Geophysics.* Elsevier [Online], 2007.

[37] Evgenya Shkolnik, G. A. H. Walker, D. A. Bohlender, P. G. Gu, and M. Kurster. Hot Jupiters and Hot Spots: The Short- and Long-term Chromospheric Activity on Stars with Giant Planets. *Astrophys. J.*, 622:1075–1090, 2005.

[38] Ian R. Stevens. Magnetospheric Radio Emission from Extrasolar Giant Planets: The Role of the Host Stars. *Mon. Not. Roy. Astron. Soc.*, 356:1053–1063, 2005.

[39] D. J. Stevenson. Planetary magnetic fields. *Earth Plan. Sci. Let.*, 208, 2003.

[40] Diana Valencia, Masahiro Ikoma, Tristan Guillot, and Nadine Nettelmann. Composition and fate of short-period super-Earths: The case of CoRoT-7b. 2009.

[41] Diana Valencia, Richard J. O'Connell, and Dimitar D. Sasselov. Internal Structure of Massive Terrestrial Planets. 2005.

[42] Brian E. Wood, Hans-Reinhard Mueller, Gary P. Zank, and Jeffrey L. Linsky. Measured Mass Loss Rates of Solar-like Stars as a Function of Age and Activity. *Astrophys. J.*, 574:412–425, 2002.

[43] P. Zarka, R.A. Treumann, B. P. Ryabov, and V. B. Ryabov. Magnetically-Driven Planetary Radio Emissions and Application to Extrasolar Planets. *Astrophys. and Space Sciences*, 277:293–300, 2001.